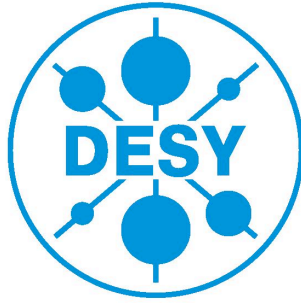


Supervisors:
Mr. Rayk Natchigall
Dr. Martin Thuczykont
Prof. Dr. Deiter Horns
HiSCORE group, Intitute for Experiemntal Physics
University of Hamburg, Germany



Air Cerenkov Detector development for HiSCORE Experiment

DESY Summer Project Report 2012

by

Sourav Sen

Indian Institute of Science Education & Research, Kolkata, India

September 6, 2012

Abstract

The mystery of the Origin of cosmic rays have perplexed mankind for a long time. Presently HiSCORE (Hundred*ⁱ Square Km Cosmic ORigin Explorer) experiment is the one being designed to look for UHE region and search for PeVatrons to solve this mystery.

This project focusses on two components of the detector development primarily. The first being an attempt to program the FPGAs in the DRS4 evaluation board (for data acquisition) which can help in customizing the detector design with more agility. For this LabVIEW FPGA module was studied. The second part of the project deals with the calibration of the gain in the PMT (the Key components of the detector) which are to be employed for the next lot of experimental prototypes in Tunka region, Russia.

Contents

1	Introduction	4
1.1	Cosmic Rays	4
1.1.1	Discovery of Cosmic Rays	5
1.1.2	Origin of Cosmic rays	6
2	HiSCORE experiment	6
3	Programming FPGA using LabVIEW	7
3.1	Introduction to FPGA	7
3.2	Classification of FPGAs	8
3.3	HDL Languages	9
3.4	LabVIEW	10
3.5	FPGA Module	10
4	Measurement of the gain of detector PMT	10
4.1	Theory	10
4.2	Gain of PMTs vs applied voltage	12
5	Conclusion	18
6	Acknowledgements	18

1 Introduction

1.1 Cosmic Rays

Cosmic Rays are highly energetic (relativistic) particles which are continually striking the earth's atmosphere from outside. Their extraterrestrial origin encapsulate in them many mysteries and informations regarding the Universe. But these cosmic rays (being mostly charged) often undergo electromagnetic interaction with the chaotic electric and magnetic fields in the interstellar medium, which engenders their trajectory to be heavily distorted and thus mystifying the source or origin in the Universe. Thus the origin of the Cosmic Rays have remained a key problem in astroparticle physics and the HiSCORE experiment is also one of the experimnts dealing with this project.

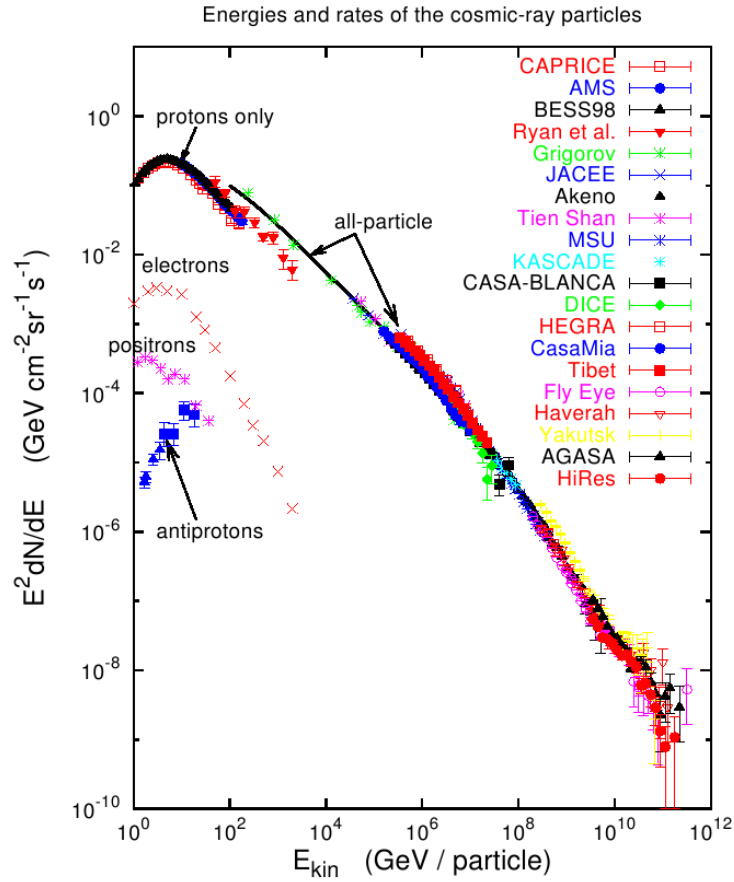


Figure 1: Spectrum of Cosmic Rays compiled from the results of several experiments [4]

1.1.1 Discovery of Cosmic Rays

After raised concerns over the discharge of ionized gases in air-tight electroscopes in the early 20th century by two Canadian groups, McLennan and Burton from the University of Toronto [1], Austrian physicist Victor Franz Hess, at the Physical Institute in Vienna deigned an experiment to investigate the sources such ionizing ray, whether they were from the Earth's crust or outer space. He released Hydrogen filled balloons in the sky and discovered that the ionization decreased with height. He concluded, that the radiation of very high penetrating power enters into the atmosphere from above [2]. After five balloon flights made during night and one during an almost total eclipse of the Sun on April 12, 1912 Hess further concluded that, since he observed no change of the rate of discharge, the Sun could not itself be the main source of the radiation.

Finally in 1925, Millikan performed experiments of submerging electroscopes in lakes at different depths and found that a depth of water equal in mass to the difference in atmospheric altitudes gave the same readings [3]. Thus it was proved that rays must come from above and he named them cosmic rays.

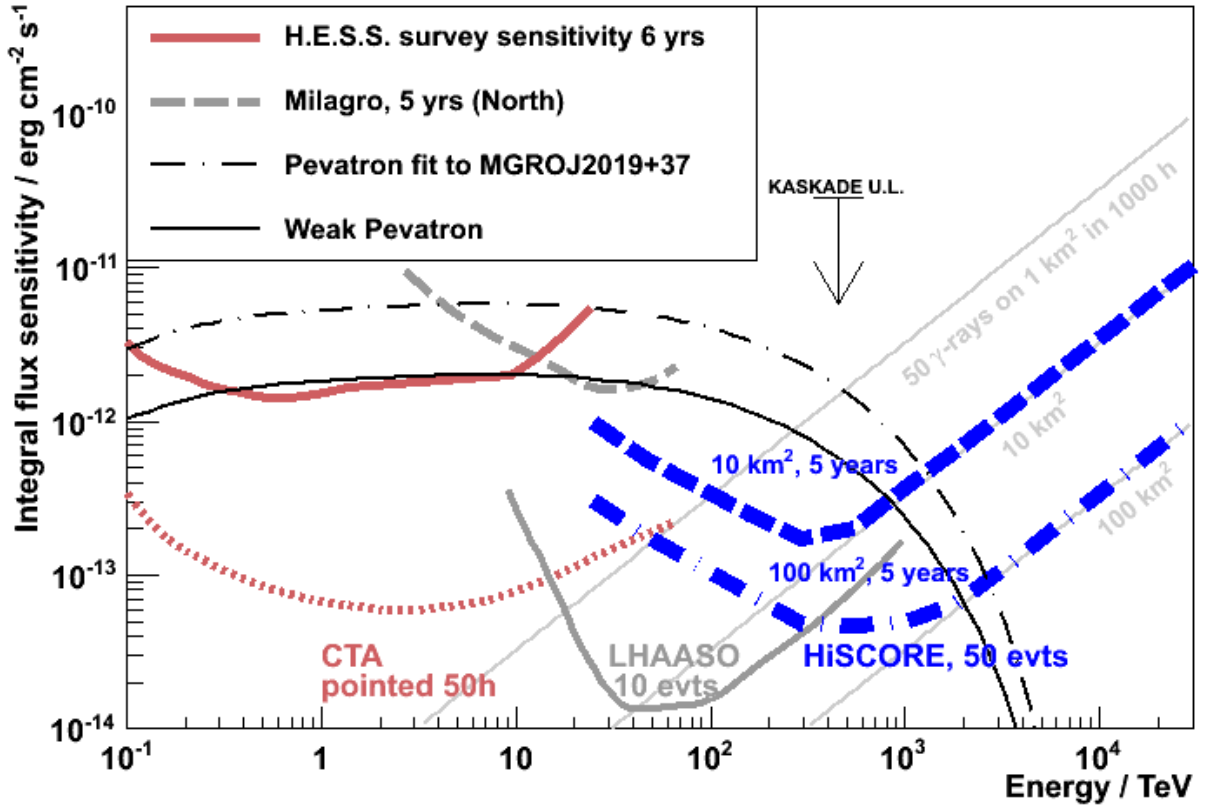


Figure 2: Energy ranges of various ground based detectors

1.1.2 Origin of Cosmic rays

Due to the unresolved ambiguity in the path of these cosmic rays a systematic study of their composition was made by several experiments to delve more into this problem. The spectrum [1] could be described by a Powerlaw above a few GeV with changes of the spectral index at 4 PeV which is called the 'knee', and at 1 EeV steeper so the 'ankle'. From the spectral study of cosmic rays it was concluded that more than 99 % of all cosmic rays are hadrons, mainly protons and helium nuclei.

The subsequent step was harness the above information about the composition of cosmic rays and envisage about possible interaction of these cosmic ray particles with the cosmic accelerator (which offers the electric and magnetic field for acceleration). Thus, it was expected that the decay of high energy mesons near the cosmic accelerators would produce accelerated neutrinos and gamma rays both of these were undeflected by the electric and magnetic fields. Hence by detecting the direction and energy of these particles, the position and nature of these cosmic rays can be understood. But cosmic neutrinos have very small interaction cross sections and thus are hard to detect and also collect enough samples for a detailed study.

The next viable option turns out to be the γ rays. They can be measured directly using satellites as well as indirectly using ground based detectors. Satellites have a constraint over their sampling area and thus they are apt for detection of low energy γ rays which have high cross-sections but not for high energy γ rays which have very low cross-section. Thus indirect ground-based detection is the only way as of now for detection of high energy γ rays. The different ground-based detectors have been displayed with their range of detection in [2]

2 HiSCORE experiment

HiSCORE (Hundred*1 Square-km Cosmic ORigin Explorer), a ground-based wide-angle (≈ 0.6 sr) large-area (100 square Km) air-shower detector for non-imaging γ -ray astronomy and cosmic ray physics from 10 TeV to 1 EeV [5], which is the ultra high energy (UHE) regime. It aims to detect thus the PeVatrons (Peta electron-Volts particles) to understand the origin of their precursor cosmic rays. It successfully achieves the goal of large instrumented area for sampling UHE γ rays as their statistics gets reduced on higher energies. It employs non-imaging detection technique of air Cherenkov radiations, which require less number of channels (less than 100 channels per km^2) as compared to imaging air Cherenkov detector arrays (over 10,000 channels per km^2).

The detector of the HiSCORE experiment consists of PMTs (see [3] which captures the Air-Cherenkov showers and pass it onto the DRS4 (Domino Ring Sampler) Data Acquisition Board which is controlled by FPGA. When four of the PMT are triggered in a threshold time, the signal is stored.

The time lag in the triggering of different detector station in the enable one to calculate the direction of the axis of the Cherenkov shower cone.

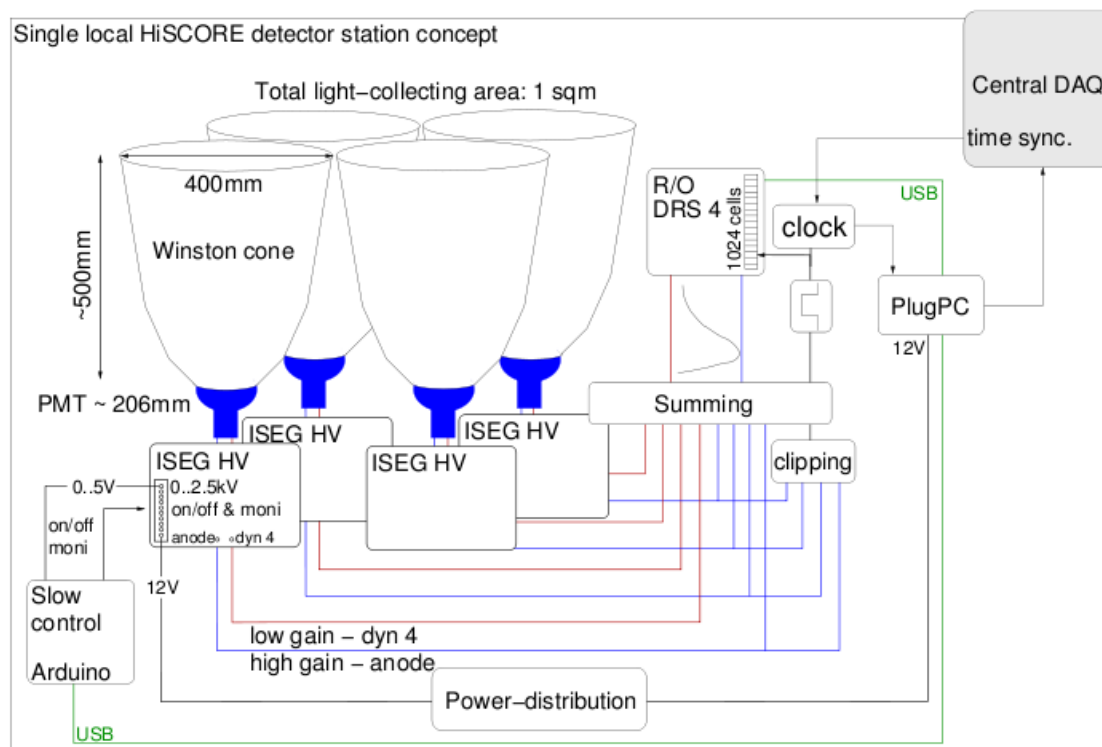


Figure 3: Schematic diagram of the HiSCORE detector

3 Programming FPGA using LabVIEW

3.1 Introduction to FPGA

FPGA stand for Field Programmable Gate Array which can be envisaged as an grid of ICs with programmable interconnections as shown in 5. FPGA consists of three basic

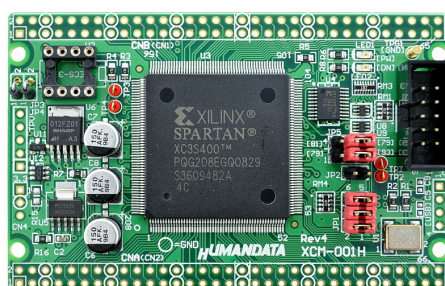


Figure 4: Evaluation Board with FPGA

component:

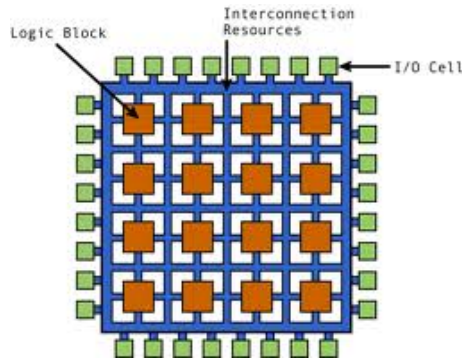


Figure 5: Schematic diagram showing the arrangement inside an FPGA

- Logic Blocks (like ICs)
- I/O Units
- Interconnections

which can be configured (or programmed) on site by the user which is why it is called 'Field Programmable Gate Array'. This feature give it an edge over ASIC (Application Specific IC), which are specially manufactured for a particular task. But still FPGA lacks in few areas like speed and bulk production cost from the conventional ASICs. Basically, user can configure the function in logical blocks (like using it as a XOR gate or an adder or the like), choose the desired I/O Units to be used and the way both these components are be interconnected (keeping in view the data flow requirement).

Since the layout of a unit cell of FPGA is repeated in a matrix form (see 5), independent data flow paths can be devised which can be executed parallely. Parallel Execution distinguishes FPGAs from microcontrollers, where a sequential order is followed while execution of the commands.

3.2 Classification of FPGAs

FPGAs differ in their architechture and functionality based on the comapanies they are manufactured from.

Currently the major FPGA vendors are:

1. Xilinx - most popular
2. Altera
3. Actel

These differ in:

- Physical means of implementing programmability

- Interconnection arrangement
- basic functionality of logic blocks

Two technologies prevailently used in FPGAs are:

- **SRAM** based Technology - Static Random Access Memory units are place at the connections and logic blocks in the FPGA grids and the are programmed to be on or off to joining or breaking a link repectively. Through this technology the memory can be flashed again and again to use them for different purposes. The Xilinx and the Altera [8] companies use this technology for their FPGAs.
- **Antifuse** tachnology - Initially in this case all the connections are switched off (open) as there is a silicon or some other insulator layer between the links. But on programming the FPGA for joining a particular link, a very voltage is passed though the link such that the insulating material starts conducting. These types of FPGAs can be programmed only once. The Actel uses this technology.

3.3 HDL Languages

FPGA are programmed using a class of programming languages called the Hardware Descriptive Languages (HDLs). There are two HDL languages 6 namely:

1. Very High Speed IC Harware Descriptive Language (VHDL)
2. Verilog Hardware Descriptive Language

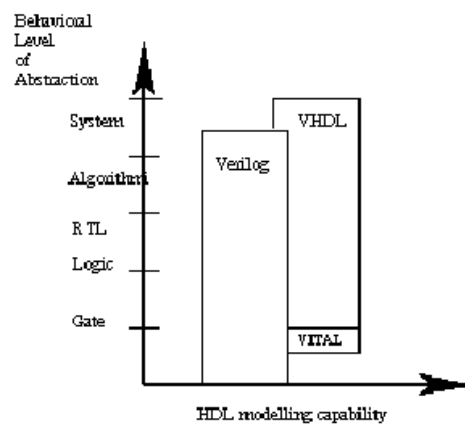


Figure 6: Comparison between VHDL and Verilog HDL

3.4 LabVIEW

LabVIEW is a system design software from National Instruments [7] for designing, implementing and testing hardware. It is like a visual programming language, where the principle behind the programming is direction of the data flow. It enables users to create flexible and scalable test, control and embedded design applications. LabVIEW projects are called Virtual Instruments (VI) which have a Front Panel and a Block diagram.

3.5 FPGA Module

- Latex converts a logic block diagram of the FPGA circuit into VHDL code and then configures the FPGA (but the code cannot be accessed) [6].
- FPGA LabVIEW module is only for Xilinx FPGAs
- It doesn't have a Verilog implementation yet
- Steps to use the module: [9]
 - Start an Empty Project and add Spartan 3E Starter Board to the host computer from Targets and Devices
 - Add the I/O resources to the Spartan 3E Starter Board
 - Now create a Spartan 3E hardware target by starting a New VI
 - Draw the Block diagram of the FPGA Board and run and download it to the FPGA Board using JTAG port

4 Measurement of the gain of detector PMT

4.1 Theory

A PMT consists of a photocathode and a series of dynodes in an evacuated glass enclosure as shown in 7. When a photon above the threshold energy strikes the photocathode, it ejects a photoelectron (due to the photoelectric effect). The photocathode material is such that the photons are produced throughout the visible region. A high voltage is applied across the cathode and anode (typically 1500 volts) and the photoelectron is accelerated towards a series of additional electrodes called dynodes. These electrodes are each maintained at successively less negative potentials. Additional electrons are generated at each dynode like an avalanche or cascading effect creates many electrons for each photoelectron for a single incident photoelectron. The amplification depends on the number of dynodes and the accelerating voltage. This amplified electrical signal is collected at the anode, which in this case is transferred to the DAQ system.

The elementary gain of a PMT can be defined as the number of photoelectrons ejected by a single photo electron in a particular dynode. This can be expressed as:

$$g = \frac{V_{sl}}{V_l} \quad (1)$$

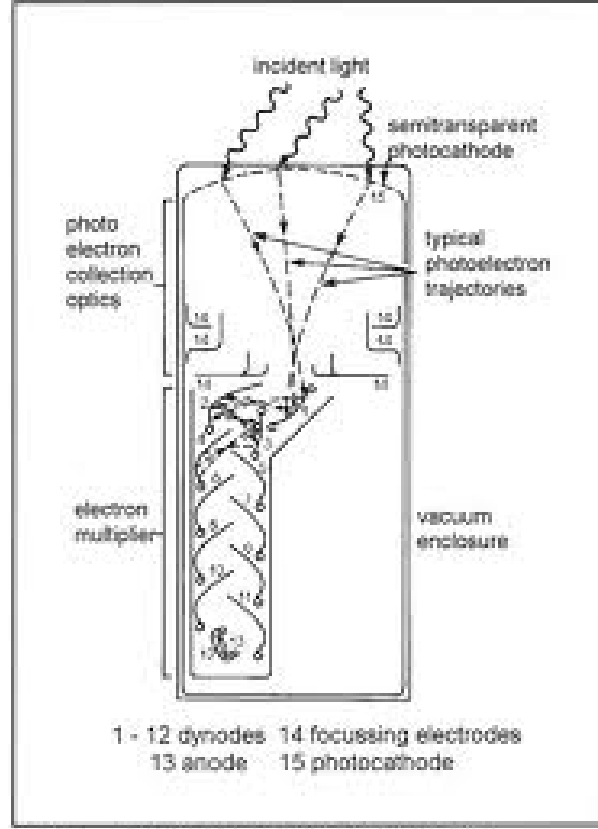


Fig. 4.1 Schematic of a photomultiplier tube.

Figure 7: Schematic of a PMT

where V_{sl} is the peak voltage measured on the second last dynode and V_l is the peak voltage on the last dynode. Also this can be expressed as:

$$g = \frac{A}{A + V_l} \quad (2)$$

where A is the anode signal.

As the apparatus uses second last dynode and the anode, gain can be expressed as:

$$g = \frac{A}{A + gV_{sl}} \quad (3)$$

which implies:

$$g = \frac{-A + \sqrt{A^2 + 4AV_{sl}}}{2V_{sl}} \quad (4)$$

Here the other solution of the quadratic equation 3 is not considered as that is not practically possible being very less.

4.2 Gain of PMTs vs applied voltage

Applied Voltage and corresponding gain of the following PMTs were measured using the set up shown in

Table 1: results for 20074

Applied Voltage (V)	Anode Signal(A)(V)	Dynode Signal(V_{sl})(V)	gain	error
980.0	-66.1947	5.7824	10.4172406383	3.06250645118
1045.0	-93.5005	10.0281	8.58652523	7.38912989782
1165.0	-151.6693	18.3021	7.13478426585	1.0175066611
1265.0	-306.4629	33.73	8.94976192778	15.2225552688
1410.0	-46.7445	3.8961	11.0462263505	4.47047118252
1590.0	-220.6069	18.9734	10.6327322484	3.3513653893
1695.0	-313.9539	23.7885	12.1259597491	1.53571283305
1765.0	-174.0574	11.5897	14.0856952503	5.09437816034
1930.0	-258.0818	16.357	14.7692367251	2.75260080412
2010.0	-294.6332	17.9153	15.5095651276	5.0993800316

Table 2: results for 20076

Applied Voltage (V)	Anode Signal(A)(V)	Dynode Signal(V_{sl})(V)	gain	error
1170.0	-126.1101	18.2425	5.70909617267	0.993761515121
1265.0	-89.7593	11.4545	6.68210388351	1.28155805036
1365.0	-146.4758	17.2263	7.39036231574	1.94133622537
1585.0	-497.492	101.8432	3.48228136362	0.181484169132
1630.0	-396.5176	33.2542	10.8999740632	2.86535389492
1715.0	-405.3687	31.44	11.8161910891	1.84691614611
1750.0	-452.9197	33.676	12.3959887061	2.7584372228

Table 3: results for 20083

Appllied Voltage (V)	Anode Signal(A)(V)	Dynode Signal(V_{sl})(V)	gain	error
790.0	-235.1636	29.3157	7.98336233657	11.8534502297
1030.0	-96.1227	11.8006	7.00632716664	1.59056686025
1260.0	-459.8397	76.1957	4.77434260671	0.536424180484
1420.0	-488.75	65.1875	6.34994838329	2.06895956257
1560.0	-464.693	57.4609	6.973554405	2.0271858694
1685.0	-494.9095	56.5504	7.66790575303	2.50284009259
1805.0	-497.2291	51.5032	8.55734265976	1.86745191912

Table 4: results for 20106

Appllied Voltage (V)	Anode Signal(A)(V)	Dynode Signal(V_{sl})(V)	gain	error
990.0	-61.3122	7.442	7.16927447984	2.92247196324
1090.0	-184.2221	25.135	7.09066378459	10.7767368683
1180.0	-269.8963	44.0763	4.8732567561	0.931165408487
1280.0	-466.5465	64.3782	6.37316082845	6.16323226707
1385.0	-402.677	50.0747	6.89226637324	1.63058101851
1480.0	-474.0485	53.6366	7.71051573257	1.26704632909
1570.0	-494.0045	47.9074	9.20411203755	1.22359600977
1655.0	-477.3797	41.0205	10.5529445468	1.58129616096

Table 5: results for 20110

Appllied Voltage (V)	Anode Signal(A)(V)	Dynode Signal(V_{sl})(V)	gain	error
995.0	-72.4614	7.0392	9.60421658859	8.16566564379
1100.0	-186.9096	24.0604	8.13647423982	16.7283326015
1270.0	-470.5501	69.1704	5.61088601873	1.59226786668
1420.0	-446.716	49.753	7.85128397959	1.53497196852
1510.0	-476.7529	50.8847	8.24686176287	1.24895814936
1595.0	-409.8664	41.1599	8.90262532146	3.09643861246
1730.0	-458.5728	37.8532	11.0259545665	1.4146225317

Table 6: results for 20112

Appllied Voltage (V)	Anode Signal(A)(V)	Dynode Signal(V_{sl})(V)	gain	error
1030.0	-121.4052	20.0016	4.84204421901	1.78398239013
1130.0	-265.3113	40.8129	5.79278567937	8.03566070157
1215.0	-457.9919	66.6606	5.70246498732	1.90253945939
1385.0	-459.2517	57.9897	6.76002704964	0.799304013584
1490.0	-465.6411	47.7049	8.63911510994	0.957530424209
1610.0	-460.6012	38.9986	10.7107445759	0.781431350235
1745.0	-467.4789	34.9032	12.3888848842	3.17689741901

Table 7: results for 20114

Appllied Voltage (V)	Anode Signal(A)(V)	Dynode Signal(V_{sl})(V)	gain	error
980.0	-58.3125	7.5122	6.65231913467	2.46772727688
1020.0	-105.17	15.4839	5.59413558742	1.31128030328
1140.0	-252.2363	32.093	8.09643044466	14.7818190884
1225.0	-259.8189	33.1422	7.54171315839	13.5790826474
1325.0	-483.2768	59.7019	6.94929158883	1.47262306491
1415.0	-494.1864	56.8689	7.55871368059	1.46809358927
1535.0	-478.1738	43.944	9.77092751144	0.612988698358
1620.0	-495.9855	41.6189	10.9588994726	4.52582802122

Table 8: results for 20125

Appllied Voltage (V)	Anode Signal(A)(V)	Dynode Signal(V_{sl})(V)	gain	error
1020.0	-78.2936	9.5186	7.49057641111	8.75833902517
1125.0	-215.9184	33.8347	5.49715535	7.25707635892
1265.0	-497.4504	80.0896	4.97150772074	1.00933856243
1390.0	-488.536	59.815	7.06633385496	2.67094604994
1540.0	-487.8121	52.2798	8.29320962901	3.00691687055
1635.0	-497.0445	51.8327	8.60443489003	4.12044883035
1770.0	-491.4282	38.6944	11.7270441765	4.41204300849

Table 9: results for 20126

Applied Voltage (V)	Anode Signal(A)(V)	Dynode Signal(V_{sl})(V)	gain	error
1040.0	-174.504	21.343	9.2909364247	18.1063587175
1105.0	-191.6069	34.7164	4.21212562822	0.769137378658
1235.0	-383.4788	63.9312	4.73161763563	0.431991310504
1325.0	-386.7574	56.4992	5.63770047166	0.99560851517
1475.0	-420.4353	50.7666	7.20570050729	2.72973748384
1540.0	-422.5473	46.855	7.8907827044	1.17666123658
1625.0	-396.936	39.4712	8.94489771971	1.22817088303
1735.0	-452.4872	38.2657	10.7852878762	2.9797939583
1865.0	-444.2161	33.378	12.2762851119	2.78181406358

Table 10: results for 20127

Applied Voltage (V)	Anode Signal(A)(V)	Dynode Signal(V_{sl})(V)	gain	error
970.0	-81.3799	7.1281	10.3687512304	2.61174795253
1030.0	-151.0033	19.6059	6.5382927546	1.23571796141
1135.0	-278.1751	36.4481	6.8326460421	6.99132934289
1285.0	-292.3167	38.6358	6.38919226225	0.785790268131
1430.0	-377.7229	42.914	7.65345404197	0.432922036842
1535.0	-384.7699	35.9516	9.62566749191	2.48867115388
1655.0	-495.9798	45.1767	9.94718460707	2.79154148243

Table 11: results for 20128

Applied Voltage (V)	Anode Signal(A)(V)	Dynode Signal(V_{sl})(V)	gain	error
985.0	-78.423	8.8553	8.17905273857	7.41077561061
1075.0	-133.8217	20.1671	8.15330645515	31.9416383312
1170.0	-114.9972	18.2051	5.10624096345	1.74212556585
1230.0	-284.7072	44.4873	5.17280648413	0.865067575963
1390.0	-257.3277	32.2068	6.82406818976	0.827699765735
1505.0	-455.9206	52.1127	7.60169688886	0.806263474436
1605.0	-305.8958	29.9412	9.10667635213	1.19627365526
1685.0	-412.0315	37.7715	9.80533819219	1.10005506524
1960.0	-319.7207	23.0064	12.8457884339	1.84834618046

Table 12: results for 20130

Appllied Voltage (V)	Anode Signal(A)(V)	Dynode Signal(V_{sl})(V)	gain	error
1090.0	-219.9158	38.9993	4.34283826892	0.593908175962
1210.0	-378.8091	61.0586	5.03294175913	2.88206430961
1385.0	-414.4136	56.1421	6.19408753834	0.539960114699
1535.0	-341.6165	36.7709	8.20450779362	2.5626610925
1615.0	-464.3592	48.7839	8.47646886974	2.90699041487
1755.0	-457.2344	39.0927	10.6828833025	2.83458152921
1955.0	-491.7429	35.1306	12.9648628972	2.76070949541

Table 13: results for 20133

Appllied Voltage (V)	Anode Signal(A)(V)	Dynode Signal(V_{sl})(V)	gain	error
1035.0	-148.1534	20.0564	7.76507837874	20.1453070741
1130.0	-298.614	47.2155	5.08191078632	0.447956333751
1265.0	-355.7248	51.2529	5.74179242609	0.914078417226
1415.0	-305.6508	35.972	7.46079647307	3.24865182607
1510.0	-345.2416	34.2403	9.03846394058	2.93206164496
1585.0	-293.9299	26.7107	9.90204603223	1.07207431058
1690.0	-253.1165	20.2318	11.4776455822	2.70064644849
1765.0	-331.018	24.7081	12.3273775656	1.65133520773
1865.0	-452.8606	31.2591	13.4382707719	2.07492015474

Table 14: results for 20138

Appllied Voltage (V)	Anode Signal(A)(V)	Dynode Signal(V_{sl})(V)	gain	error
990.0	-85.4682	12.5438	5.61183247732	1.13274888982
1015.0	-108.3184	16.6835	5.30837899838	2.04095543299
1055.0	-188.0927	28.9932	5.8445044611	10.058276738
1080.0	-227.274	31.4671	6.83000260058	9.92882781525
1135.0	-405.8328	59.3153	5.82679890061	4.44370045783
1340.0	-492.1039	62.956	6.64572492987	0.731696722707
1415.0	-446.86	53.9786	7.11891347282	0.612094685741
1510.0	-483.4266	55.3017	7.63471526979	1.86162809518
1650.0	-391.6844	33.8196	10.4935391862	1.59017731093
1710.0	-487.9441	40.9491	10.8815324002	2.68153315306
1835.0	-418.4569	29.3378	13.2105869077	1.8439536415
1915.0	-444.7553	28.9198	14.3269715077	1.77205951522
1985.0	-482.5943	31.2078	14.4770585211	3.35411715523

Table 15: results for 20139

Appllied Voltage (V)	Anode Signal(A)(V)	Dynode Signal(V_{sl})(V)	gain	error
1015.0	-80.8058	10.0543	6.91786626557	2.10617673655
1135.0	-223.9904	31.4923	6.54028380025	9.2720885962
1260.0	-494.7027	69.406	6.06358968517	3.61649304839
1420.0	-480.918	57.2803	7.23908007311	0.582508384918
1535.0	-444.5263	48.9415	7.94465078296	0.786488440925
1625.0	-448.2112	48.2821	8.21224089606	2.35663986287
1830.0	-453.7056	34.5192	12.0696801802	1.50352994231

Table 16: results for 20141

Appllied Voltage (V)	Anode Signal(A)(V)	Dynode Signal(V_{sl})(V)	gain	error
985.0	-68.8509	4.9454	13.7447666232	14.3633082188
1030.0	-106.8684	8.44	11.8641642808	6.96218238241
1115.0	-202.3048	18.9774	13.9711366806	33.6869645723
1265.0	-314.4478	37.5785	7.72991513372	9.49814701908
1430.0	-304.1533	35.5325	7.41387748401	1.23076817947
1520.0	-370.5246	41.3653	7.81702572442	0.79616545849
1625.0	-425.034	41.0284	9.2425635662	0.664159234932
1745.0	-468.6443	40.0667	10.6508562316	2.86577808738

Table 17: results for 20149

Appllied Voltage (V)	Anode Signal(A)(V)	Dynode Signal(V_{sl})(V)	gain	error
1015.0	-55.8189	6.7489	7.24395725348	3.826696769
1110.0	-151.1117	21.1057	7.37964173674	19.0299119198
1265.0	-422.7125	68.0437	5.00280882582	2.25766301208
1520.0	-491.6616	52.4543	8.2666268724	1.69118484237
1610.0	-466.4055	50.3017	8.20124678586	2.64160189137
1770.0	-496.8581	44.9219	9.98943696951	2.14510836609

Table 18: results for 20149

Appllied Voltage (V)	Anode Signal(A)(V)	Dynode Signal(V_{sl})(V)	gain	error
1015.0	-89.4032	13.509	5.48013082857	2.99939493584
1120.0	-168.1149	24.0403	8.36713897184	23.9666565992
1280.0	-497.2619	75.6371	5.35834431966	1.05942274904
1390.0	-494.1112	62.7164	6.71024150112	0.805105438606
1510.0	-406.0937	46.528	7.59371081293	1.32197461652
1605.0	-457.5341	46.3125	8.75853490846	0.910447503251
1765.0	-471.1518	38.0745	11.395427673	3.42596181342

5 Conclusion

The project has undertaken to aid in the development of the prototype detector for the HiSCORE experiment to be instrumented at the Tunka Region, Russia. The author was involved in devising convenient ways to program FPGA to be extensively used in the Data Acquisition system. For this the LabVIEW FPGA module was investigated. It led to a partial success, though due to time constraint, the ultimate goal of programming the DRS4 evaluation board for the experiment could not be accomplished. Author also dealt with the calibration the fundamental gain with the applied voltage on 19 PMTs (1 was damaged in the process) which were to be used in installing 5 new prototype detector stations in the Tunka Region.

6 Acknowledgements

I convey my deepest gratitude to Mr. Rayk Natchigall, Intitute for Experimental Physics, University of Hamburg, Germany for offering me a project in the HiSCORE group and for his cooperative attitude, appreciations and valuable guidance during every step of the project.

I owe a great debt of gratitude to Dr. Martin Thuczykont, Intitute for Experimental Physics, University of Hamburg, for ungrudging help, affectionate guidance, constant encouragement throughout the course of this project work and his incredible patience in molding this piece of project.

I deem it to be my humble privilege to express my esteem sense of gratitude and unforgettable indebtedness to Prof. Dr. Deiter Horns,, Intitute for Experimental Physics, University of Hamburg, for his valuable guidance and encouragement throughout my project.

I extend my hearty gratitude to Mr. Ulrich Einhaus, Mr. Michael Bu"ker for their help during the project and for their wonderful company during my whole stay in DESY. I would like to thank all the group members of the Experimental Astroparticle Physics group, Universty of Hamburg for providing me such a friendly and conducive environment for carrying my project that made my summer research experience wonderful.

I wish to thank Prof. Olaf Behnke and other in Deutsches Elektronen-Synchrotron (DESY), Hamburg for organizing such a great summer programme and for all the enriching lecturesdurng the programme.

I am lucky to meet my fellow summer students in this programme and had great friends. I would like to extend my gratitude to Prof. Amitava Datta, IISER Kolkata and Prof. R N Mukherjee, Director, IISER Kolkata for encouraging me to join this programme. I am highly indebted to my parents for their constant encouragement and support.

References

- [1] McLennan, J.C. and Burton, E.F.:Physical Reviews **184** (1903).

- [2] Hess, V.F.: *Physikalische Zeitschrift* **13**, 1084 (1912).
- [3] Millikan, R.A.: *Proceedings of the National Academy of Sciences* **12** (1926).
- [4] Cronin, J. et al.: *Scientific American* **276**, 44 (1997).
- [5] Thuczykont, M. et al.: arXiv:**1108.5880** [astro-ph.IM].
- [6] LabVIEW FPGA Module User Manual
- [7] National Instrument site: <http://www.ni.com/>
- [8] Altera site: <http://www.altera.com/>
- [9] <http://lnr.irb.hr/pd/daqws/images/V.Petousis.pdf>